

Cyclical oscillations and absorbing-state probabilities in optional public goods games: Interplay of reward and group size

Eduardo V. Stock^{1,*}, Pablo Valverde^{2,†}, Juan Carlos González-Avella^{3,‡}, José Roberto Iglesias^{1,4,§},
Sebastian Gonçalves^{1,||} and Roberto da Silva^{1,¶}

¹*Instituto de Física, Universidade Federal do Rio Grande do Sul, Caixa Postal 15051, 91501-970 Porto Alegre RS, Brazil*

²*Pontificia Universidad Católica del Ecuador, Facultad de Ciencias Exactas y Naturales, Quito 170525, Ecuador*

³*Institute for Cross-Disciplinary Physics and Complex Systems, UIB-CSIC, Palma de Mallorca 07122, Spain; Advanced Programming Solutions SL, Palma de Mallorca 07120, Spain*

⁴*Instituto Nacional de Ciência e Tecnologia de Sistemas Complexos, CBPF, Rio de Janeiro 22290-180, RJ, Brazil*



(Received 28 September 2024; accepted 18 December 2024; published 21 January 2025)

The optional public goods game (OPGG) is a three-strategy model in which individuals can cooperate, defect, or not participate. Despite its simplicity, this model effectively captures various social dilemmas, including those involving public services, environmental sustainability, and broader societal issues. In this study, we investigate how the reward (r) and group size of potential players (S) of public goods games influence the steady-state coexistence of these strategies or the alternation of their dominance in a rock-paper-scissors dynamic. The OPGG is simulated using Monte Carlo in a nonspatial scenario, meaning there is no topology connecting the agents, allowing any player to interact with any other player. We show that under sufficiently noisy conditions, the system consistently evolves to an absorbing state, with the prevailing strategy determined by the values of r and S . In the range $2 \leq r \leq S$, the system shows multiple stable absorbing states, with groups of size $S = 4$ exhibiting more pronounced and transient rock-paper-scissors dynamics with longer average absorbing times. We present a thorough analysis of our results in terms of the fraction of time the system spends in rock-paper-scissor cycles, the number of cycles, and the average probability that the system relaxes to each possible absorbing state, including scenarios where the system does not reach an absorbing state at all.

DOI: [10.1103/PhysRevE.111.014138](https://doi.org/10.1103/PhysRevE.111.014138)

I. INTRODUCTION

The natural emergence of cooperative behavior among independent individuals has been a major focus of both biological and social research [1,2]. This interest is driven by humanity's pressing challenges—such as resource depletion, pandemics, and global warming—that rely on cooperative efforts for resolution. To address these challenges, researchers seek to uncover the fundamental mechanisms within systems of interacting agents that foster cooperation.

A key focus in this field is to understand how agents perceive their roles and gains within a system. For example, studies have shown that an agent's perception of fairness can determine whether a system evolves toward full cooperation or complete defection under specific conditions [3]. Additional research has explored various factors influencing cooperation, including individual absolute and relative gains [4], payoff-based learning [5], cost- and benefits-based learning [6], conditional cooperation [7–9], conditional

defection [10], behavioral strategies and reputation [11], among others [12–14].

A significant portion of researchers strive to understand not only what causes cooperation to emerge but also what enables it to persist over time [15–19]. This effort is driven by the nearly inevitable emergence of free riding [7,20]—where individuals exploit the collective effort of others for personal gain, even when universal cooperation would result in greater benefits for everyone. While mechanisms such as central punishment [21–23], peer-to-peer punishment [24], and rewards [25] can foster cooperative behavior, they often rely on the ability to identify and target individuals effectively [26].

To understand the promotion of cooperation in various systems, several mechanisms in different topologies have been proposed, such as information sharing between players [27], agents' spatial diffusion on lattices [28], punishment and adaptation in regular graph social dilemmas [29], conditional dissociation of defectors [14], and higher-order interactions between players in complex networks [30]. For instance, Ma *et al.* demonstrated that cycles of cooperation and free riding can emerge in social systems, with free riders and cooperators varying periodically depending on the community size and individual costs of cooperation and defection [31].

Among the standard game-theoretic models used to describe social dilemmas [32], where private and collective interests appear to conflict, is the public goods game (PGG). The PGG is defined as a game where players are given the

*Contact author: eduardo.stock@ufrgs.br

†Contact author: pblvalverde@gmail.com

‡Contact author: avellaj@gmail.com

§Contact author: iglesias@if.ufrgs.br

||Contact author: sgonc@if.ufrgs.br

¶Contact author: rdasilva@if.ufrgs.br

opportunity to invest their money in a shared fund, with profits or gains of any kind distributed equally among all participants, regardless of individual contributions. Ideally, it might seem fair for individuals with similar financial means to contribute equally to these projects. However, people differ in their social and financial circumstances, meaning that some can afford to invest more than others. One possible reason purely rational players choose to invest nothing is that they may not be fully aware of others' contributions, leading them to defect for short-term gain, even though this behavior ultimately contributes to collective economic decline.

Among the various approaches to the PGG, one of the earliest involves studying a single pool where players interact and contribute to a shared public good. The dynamics of this system are shaped by motivation, as modeled by some authors [33–36]. This approach became widely known in the context of evolutionary computing as the public investment game (see, for example, Ref. [33]). In contrast, other authors propose scenarios where agents participate in multiple groups or contribute to separate pools [37], introducing more complex interaction dynamics.

An important contribution to the PGG model was made by Hauert *et al.*, where the authors showed that voluntary participation in the PGG introduces abstention as a stabilizing mechanism, allowing cooperators and defectors to coexist [38]. This variation is denoted as optional public goods game (OPGG) and serves as a valuable model for understanding social conflicts and activities where cooperation is essential but voluntary, allowing players that do not want to be exploited to opt out. A real-life example where a type of OPGG can be observed is in the context of voluntary climate action and sustainability efforts, where cooperators are those who actively participate in sustainable practices, such as recycling or reducing emissions, to benefit the environment. Defectors choose not to contribute but still enjoy the cleaner environment that cooperators help create. Meanwhile, other players neither contribute to nor benefit from these efforts, often isolating themselves from environmental initiatives. In the OPGG, players who choose to abstain from participating in the game, receive a fixed payment, and become the so-called loners.

The coexistence of the three strategies: cooperators (C), defectors (D), and loners (L), as well as the cyclical dominance [39] among them [i.e., rock-paper-scissors (RPS) dynamics], has been identified as a possible outcome of the OPGG when analyzed using mean-field replicator dynamics [40,41]. These findings are significant, as both equilibrium and cyclic dominance scenarios suggest the spontaneous emergence of cooperation.

However, these results were demonstrated to emerge only for specific parameter ranges. A comprehensive analysis across a broader set of parameters that promote cooperation has yet to be conducted and warrants further investigation. Questions about the statistics of the number, size, and duration of cycles are essential for a complete understanding of the problem. Therefore, an alternative numerical study of the OPGG model is necessary, along with numerical simulations that relax the assumptions used in the mean-field regime.

Two critical factors influencing public goods games are the multiplication factor of the common pool and the size of sample groups of potential players. The multiplication factor has consistently been shown to enhance cooperation (e.g., Refs. [42,43]), whereas the impact of group size remains debated. Larger groups are sometimes seen as less cooperative due to coordination challenges [44,45], while others suggest that they foster cooperation through increased diversity and resource pooling [46,47]. Despite extensive studies of group size effects in public goods games, both experimentally [47] and theoretically [46,48], there remains limited understanding of how these factors influence the OPGG.

In this paper, we present a comprehensive analysis of the OPGG through simulations, exploring conditions for the emergence of spontaneous cooperation. We examine whether cooperation arises as coexistence in steady equilibrium states or as alternating dominance among strategies in a rock-paper-scissors manner. Our analysis focuses on the simultaneous effects of the multiplication factor (r) and sample group size (S) on the outcomes of the OPGG, addressing gaps in the literature and shedding light on how these two key parameters influence the dynamics of spontaneous cooperation in communities with no topological structure. In Sec. II, we describe the model and the results are presented in Sec. III. The summaries and conclusions are given in Sec. IV.

II. MODEL

We consider a population of N agents that can be found in one of three possible states: C (cooperator), D (defector), or L (loner). The OPGG evolves as follows:

- (i) Two different agents, here denoted as i and j , are randomly chosen from the population.
- (ii) For each of the chosen agents, a set of $S - 1$ distinct agents are randomly selected (uniform distribution) from the $N - 1$ agents left giving rise to two groups: S_i and S_j . Both groups can share one or more agents.
- (iii) Each cooperator in a group contributes to the common pool with a unit of wealth. Defectors participate, but without contribution, while loners stay out of the game and expect a fixed payoff σ of his/hers unit of wealth invested.
- (iv) Payoffs are then calculated for the three strategies:

$$P = \begin{cases} \frac{rN_C}{(N_C+N_D)} - 1 & ; C \\ \frac{rN_C}{(N_C+N_D)} & ; D \\ \sigma & ; L \end{cases}, \quad (1)$$

where r is the multiplication factor of the public good, N_C , N_D , and N_L are the numbers of cooperators, defectors, and loners, respectively, in the local configuration.

(v) With complete knowledge of S_i and S_j payoff information, agent i chooses to switch to player j strategy according to a transition probability only inspired by Glauber dynamics (or Fermi-Dirac rule as referenced by other authors in the literature), within the context of spin systems:

$$P_{i \rightarrow j} = \frac{1}{1 + e^{-(P_j - P_i)/k}}, \quad (2)$$

where k is a parameter that measures the level of randomness in the strategy-switching dynamics [49,50].

(vi) The steps above are repeated N times to make one Monte Carlo step.

The sequential strategy imitation approach, adhering to the transition probabilities described in Eq. (2), was chosen, as in Refs. [50,51], for its flexibility in capturing a wide spectrum of stochastic behaviors across two distinct scenarios: agent's deterministic change of strategy and purely random strategy switching with intermediate level randomness in between, which was shown to be important to promote cooperation [9].

In the limit $k \rightarrow 0$, player i adopts the strategy of player j if $P_i < P_j$ and retains his or her own strategy otherwise. In this regime, randomness arises only in the case where $P_i = P_j$, with player i changing strategies with a probability of $1/2$. On the other hand, when $k \rightarrow \infty$, players exhibit a $1/2$ probability of changing or retaining their strategy, irrespective of the payoff differences between them.

Between these two extremes, the sequential strategy imitation mechanism provides a continuum of stochastic levels, offering varied levels of randomness and adaptability. To investigate the collective dynamical behavior of the system, we follow the state of the system by measuring the fraction (or density) of individuals in the three possible strategies, $\rho_C^{(l)} \equiv \frac{N_C^{(l)}}{N}$, $\rho_D^{(l)} \equiv \frac{N_D^{(l)}}{N}$, and $\rho_L^{(l)} \equiv \frac{N_L^{(l)}}{N}$, cooperators, defectors, and loners, respectively, at a given time step l .

Under specific conditions, the system can exhibit a dynamic state where the dominant strategy changes in a steady, cyclic manner, commonly referred to as rock-paper-scissors (RPS) cycles. In our case, the cooperator-defector-loner (CDL) cycle is a more suitable descriptor (or equivalently, LCD, or DLC). We will use the terms RPS and CDL interchangeably to describe instances of cyclic switching strategies. We will denote the number of complete cycles within a specified time frame by λ . Another important variable for measuring the occurrence of RPS cycles was proposed in Ref. [28], and it is defined as:

$$\alpha \equiv \frac{1}{t_f} \sum_j t_j, \quad (3)$$

where t_j is the duration of the j th RPS cycle. The quantity α measures the time fraction of the RPS cycles within the evolution time frame t_f .

To better understand how λ and α are measured, we recall that during a cooperator-defector-loner (CDL) cycle, one strategy (X) prevails over the others. This is expressed as $\rho_X^{(l)} > \rho_{Y,Z}^{(l)}$ (the density of agents using strategy X is greater than the density of agents using the other two strategies at time step l). Thus, if, within a given time interval, the dominant strategies follow the sequence:

CDDLLL-CCDDLL-CDDLLLLL-DL,

where the last prevalent strategy in the sequence is L shown in bold, then the number of complete RPS cycles is $\lambda = 3$ and the time fraction with RPS cycle occurrence within the given timeframe is $\alpha = (6 + 6 + 8)/22 \approx 0.91$. As one might think, λ scales with time, while α does not.

In the next section, we present the main results obtained via Monte Carlo simulations. For clarity, in this work, we only

studied initial conditions where all strategies were equally likely to happen, i.e., $\rho_C^{(0)} = \rho_D^{(0)} = \rho_L^{(0)} = 1/3$. We also considered the payoff of the loner strategy to have a fixed value of $\sigma = 1$, so there is no further reference to it in this work.

III. NUMERICAL SIMULATIONS

We first show four typical behaviors of the OPGG model by presenting the evolution of the fraction of cooperators, defectors, and loners for different values of the multiplication factor r , while keeping the other parameters fixed at $S = 5$ (group size) and $k = 0.1$ (noise). Figure 1(a) shows that after a few MC steps, the system reaches an absorbing state where all agents adopt the loner strategy ($\rho_L = 1$) for $r = 1$; this is expected because, with $r = 1$, the loner's payoff is always greater than that of the other strategies. In contrast, for $r = 2.5$, Fig. 1(b) shows that the evolution reaches a steady state where all strategies coexist, with small fluctuations around their mean values. Then, for $r = 3.5$, the three strategies still coexist, but the collective behavior of the system changes drastically, as can be seen in Fig. 1(c). The dynamics now present large oscillations, with the prevalent strategy changing cyclically corresponding to the emergence of RPS cycles. Finally, in Fig. 1(d) we show that for a sufficiently large return, i.e., $r = 5$, the system presents major fluctuations as cooperators and defectors endures in a struggling dynamics before reaching an absorbing state where all players defect. As noted in Ref. [40], full cooperation is expected to happen for $r > S$, once there is no more social dilemma, however, there is a transition for $r = S$, where cooperators and defectors coexist for longer as the payoff of both strategies tend to equality.

The presence of RPS cycles shown in Fig. 1(c) for the specific set of parameters is in agreement with the results obtained by Hauert *et al.* [40], using replicator dynamics. To further investigate the presence of RPS cycles, we conducted three independent runs (with different random seeds), as presented in Fig. 2, using parameters $N = 10^4$, $r = 3.5$, and $k = 1$. We observe that all three runs exhibit RPS cycles with large oscillations but with different durations until the absorbing state of defection is reached.

The absorbing time, denoted as τ , is the time at which the system reaches an absorbing state ($\rho_X^{(l)} = 1$) and remains fixed as all other strategies become extinct. We infer that τ , along with the RPS cycle time fraction (α), the number of RPS cycles (λ), and the final absorbing state, are random variables whose expected values (and higher moments) probably depend on the parameters r , S , and k that govern the dynamics.

To better characterize the situation described above, we define estimators for the probabilities of the system reaching each of the three possible strategies as an absorbing state, as well as not reaching an absorbing state at all. Here, we denote the estimator to reach a strategy X as π_X , where $X = C, D$, or L , and define it as

$$\pi_X \equiv \frac{1}{N_{\text{run}}} \sum_i \xi_X^{(i)}, \quad (4)$$

where

$$\xi_X^{(i)} = \begin{cases} 1, & \text{if simulation reached absorbing state } X, \\ 0, & \text{else.} \end{cases} \quad (5)$$

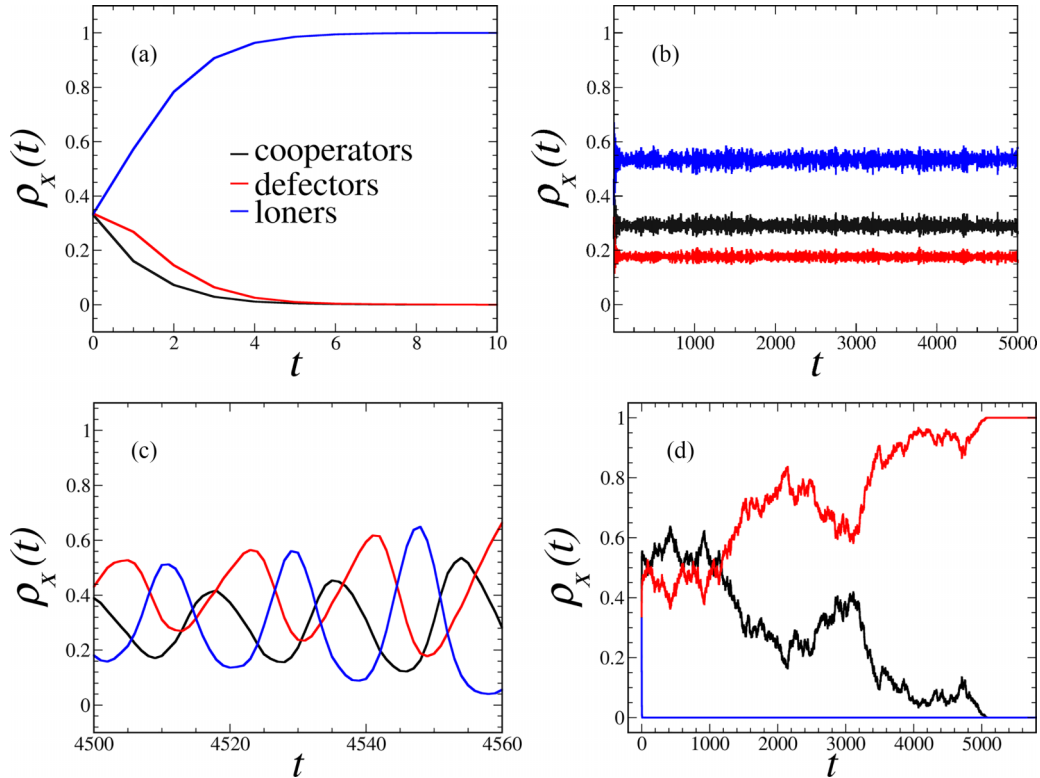


FIG. 1. Evolution of the fraction of cooperators, defectors, and loners for (a) $r = 1$, (b) $r = 2.5$, (c) $r = 3.5$, and (d) $r = 5$. Each time series was obtained with $N = 10^4$ (total population size), $S = 5$ (group size), and $k = 0.1$ (noise level).

The estimator [Eq. (4)] is calculated by summing the runs (with different seeds) that resulted in an absorbing state of the strategy X , divided by the total number, N_{run} . If $\tau \rightarrow \infty$, it indicates a nonabsorbing steady state, which is not computationally feasible. To overcome this, we set a maximum simulation time of $t_{\text{max}} = 10^5$ MC steps. If the system does not reach an absorbing state by then, we consider $\xi = 0$. This scenario contributes to the nonabsorbing state, where the estimator is given by:

$$\bar{\pi} \equiv 1 - \sum_X \pi_X. \quad (6)$$

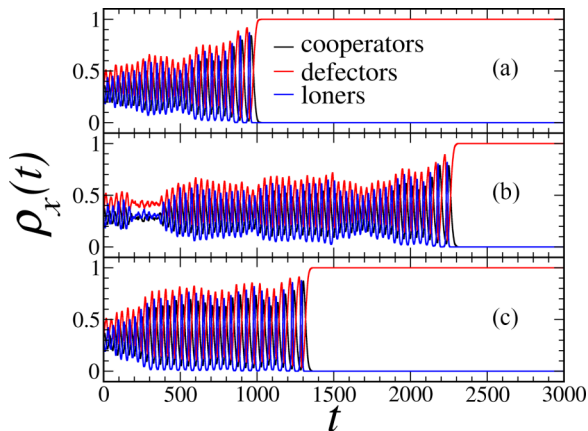


FIG. 2. Evolution of the strategies densities for $r = 3.5$ of three runs with the same parameters $N = 10^4$ (system size), $S = 5$ (group size), and $k = 1$ (noise level) but different initial random seeds.

In such cases, we do not compute a value for τ , but we do measure α , which is straightforward to define as $t_f = t_{\text{max}}$ [see Eq. (3)].

A. Population size effects (N)

A key aspect of our analysis is to determine the finite-size scaling of the dynamics. In the mean-field approach in Ref. [40], the population from which groups of agents are sampled and invited to participate in a public goods game must be sufficiently large and well mixed. Thus, for $S = 8$ and $k = 1$, we investigate how different population sizes (N) affect the average absorbing times (τ), the occurrence of RPS cycles (α and λ), and the probability of reaching each possible steady state. We studied the expected values and standard deviation of τ , α , λ , and π as a function of r in the range $r \in [1, 10]$, where each point was obtained from $N_{\text{run}} = 10^4$ samples (time series with identical parameters but different seeds). We fixed the maximum simulation time at $t_{\text{max}} = 10^5$ MC steps, as previously stated, which means that the simulation ends if no absorbing state was reached until then.

In Fig. 3, we show the results for $\langle \tau \rangle$ [Fig. 3(a)], $\langle \alpha \rangle$ [Fig. 3(b)], and $\langle \lambda \rangle$ [Fig. 3(c)]. In Fig. 4, we show the results for the steady-state estimators where we use the symbol π (without bar or subscript) to indicate the probability of reaching any possible steady state (absorbing or not). The first thing we notice in Figs. (3a)–(3c) is that the results become more prominent as larger systems are considered. Similarly, in Fig. 4, we observe a finite-size scaling through π as the boundaries of the region where $2 \lesssim r \lesssim 8$ show an abrupt crossover of loners to cooperators at $r \approx 2$ and defectors to

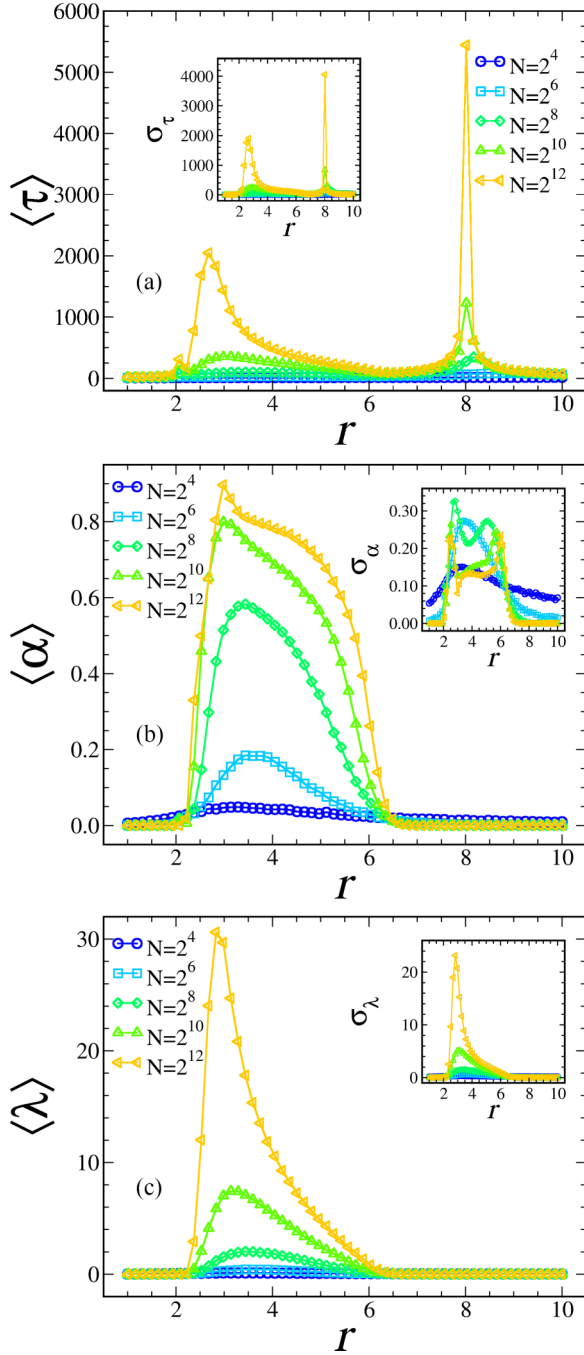


FIG. 3. Study of the system size considering a fixed sample group size $S = 8$. We show (a) the average absorbing time, (b) the average time fraction with RPS cycles, and (c) the average number of cycles within the simulation time span as functions of r . Each point was obtained from a sample size of $N_{\text{run}} = 10^4$.

cooperators when $r = 8$. As another general remark, within this region, we can identify a range of mixed dynamics with multistability of the absorbing state occurring in more narrow intervals of the vicinity of $r = 3$ as larger systems are considered.

Additionally, for $r \gtrsim 2.5$ we start to observe the emergence of RPS cycles as larger populations are taken into account, as shown in Figs. 3(b) and 3(c), suggesting that larger systems

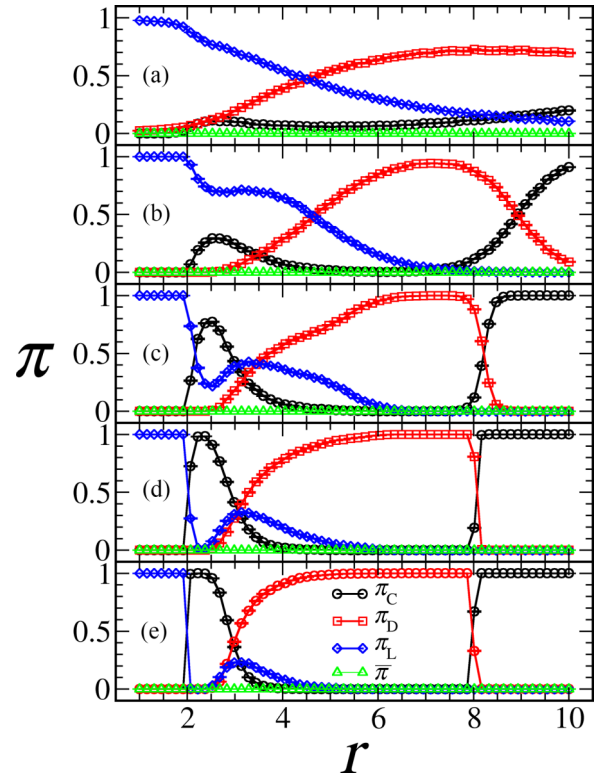


FIG. 4. Probabilities of reaching an absorbing state (or not) as a function of r , for different system sizes (a) $N = 2^4$, (b) $N = 2^6$, (c) $N = 2^8$, (d) $N = 2^{10}$, and (e) $N = 2^{12}$ for fixed $S = 8$. Each point was obtained by averaging over 10^4 runs.

provide a more favorable environment for the occurrence of RPS cycles. The maximum peak of $\langle \alpha \rangle$ shifts slightly from $r \approx 3.5$ to $r \approx 3$ as the population increases from $N = 2^6$ to $N = 2^{12}$, as we can see in Fig. 3(b). Furthermore, it can be observed in Fig. 3(a) that RPS cycles are sustained for longer periods in larger systems. For instance, when comparing $N = 2^{10}$ and $N = 2^{12}$, the peak of the average number of cycles ($\langle \lambda \rangle$) increases approximately by a factor of 3, while $\langle \tau \rangle$ increases approximately by a factor of 10 at its peak. Again, the increase in the average RPS time fraction from $\langle \alpha \rangle \approx 0.8$ to $\langle \alpha \rangle \approx 0.9$ reinforces the conclusion that RPS cycles persist for extended durations in larger systems.

In parallel, we note that the estimators π present a more complex scenario within the region $2 \lesssim r \lesssim 8$ than the results of Fig. 3 might suggest. Studying the case of $N = 2^{12}$, we begin by looking at the vicinity of $r = 2$, we observe that the system crosses over abruptly from a certain absorbing state of loners ($\pi_L = 1$) to a certain steady state of cooperators, maintaining this cooperative trend until $r \approx 2.5$. Beyond this point, multistability emerges as the other two strategies gradually become more likely absorbing states, reaching a regime around $r \approx 3$ where the system is almost equally probable to relax to cooperator, loner, or defector. Interestingly, every single run in the sample reached an absorbing state for the parameters studied, as shown by the green curves in Fig. 4 ($\bar{\pi} = 0$). This suggests that the stochasticity level of the strategy-switching dynamics (k) is seemingly high enough to prevent the system from resting in a steady state of coexistence.

Finally, when $r \approx 8$, we observe in Fig. 4 that the system presents another abrupt crossover by switching from the known defector's economic stalemate as free riders take over the dynamics to a scenario where the public goods game reward (r) is sufficiently high to allow the cooperation to be the most profitable strategy even if free riding is still a valid strategy. This crossover is also reflected in the average absorbing time ($\langle \tau \rangle$), which shows a peak for $r \approx 8$ as we can observe in Fig. 3(a). This specific finding aligns remarkably well with the results of the replicator dynamics approach discussed in Ref. [40]. In the next section, we discuss the underlying reasons behind this alignment as we present our study results on the influence of sample group sizes (S).

B. Sample group size effects (S)

We now show the sample group size study and show how it affects the emergence of RPS cycles and the overall system dynamics. In this analysis, we fixed the population at $N = 2^{13}$ and the noise parameter at $k = 1$, and studied how the measurements ($\langle \tau \rangle$), $\langle \alpha \rangle$, $\langle \lambda \rangle$, and π change as a function of r for different sample group sizes. In Fig. 5(a), we show the average time to reach the absorbing state. We observe that the system transitions from a regime with short absorbing times for $S = 2$, where the absorbing time does not depend on the OPGG reward r , to a sharp increase beginning around $r \approx 2$ for $S = 2^2$. For this group size, a maximum average time of approximately 25×10^3 MC steps to reach an absorbing state. Interestingly, for larger sample groups, such as $S \geq 2^3$, $\langle \tau \rangle$ decreases compared to $S = 2^2$, indicating that some mechanism in smaller groups is responsible for sustaining the dynamics for much longer.

The longer duration of the evolution towards an absorbing state occurs because the RPS cycles are more likely to occur with smaller groups, as we can see in Fig. 5(b), where we show the average fraction time with RPS cycles. Cooperation seems to persist longer within RPS cycles in contrast to Ref. [52]. We observe that in the same manner that $\langle \tau \rangle$ shows a spike for $S = 2^2$, $\langle \alpha \rangle$ also has a maximum value for the same group size, but $\langle \tau \rangle$ shows its peak at $r \approx 2.5$, while $\langle \alpha \rangle$ shows to be maximum at $r \approx 2.8$. However, for larger group sizes such as $S = 2^3$ and $S = 2^4$, we observe that the RPS cycles are kept for higher values of r , even if it is for shorter times, as shown in Fig. 5(a). As a complementary result, we show in Fig. 5(c), that the average number of RPS cycles also shows rapid growth in the interval $2 \lesssim r \lesssim 3$ when considering sample groups of size $S = 2^4$.

Finally, in Fig. 6, we present the probabilities of the system reaching or not reaching an absorbing state, that is, π , as a function of r for sample group sizes (a) $S = 2$, (b) $S = 2^2$, (c) $S = 2^3$, and (d) $S = 2^4$ using the same set of parameters as in the previous results.

As an overview, the system shows the clear behavioral pattern divided into three distinct regions as previously seen in Fig. 4. Here, however, it has a more pronounced dependence on S . For values of $r \leq 2$, the system settles consistently in an absorbing state dominated by loners. When $r \geq S$, the system relaxes into a stable state of cooperators. In the intermediate range, where $2 < r < S$, changes in the likelihood of the system reaching a specific steady state become more abrupt for

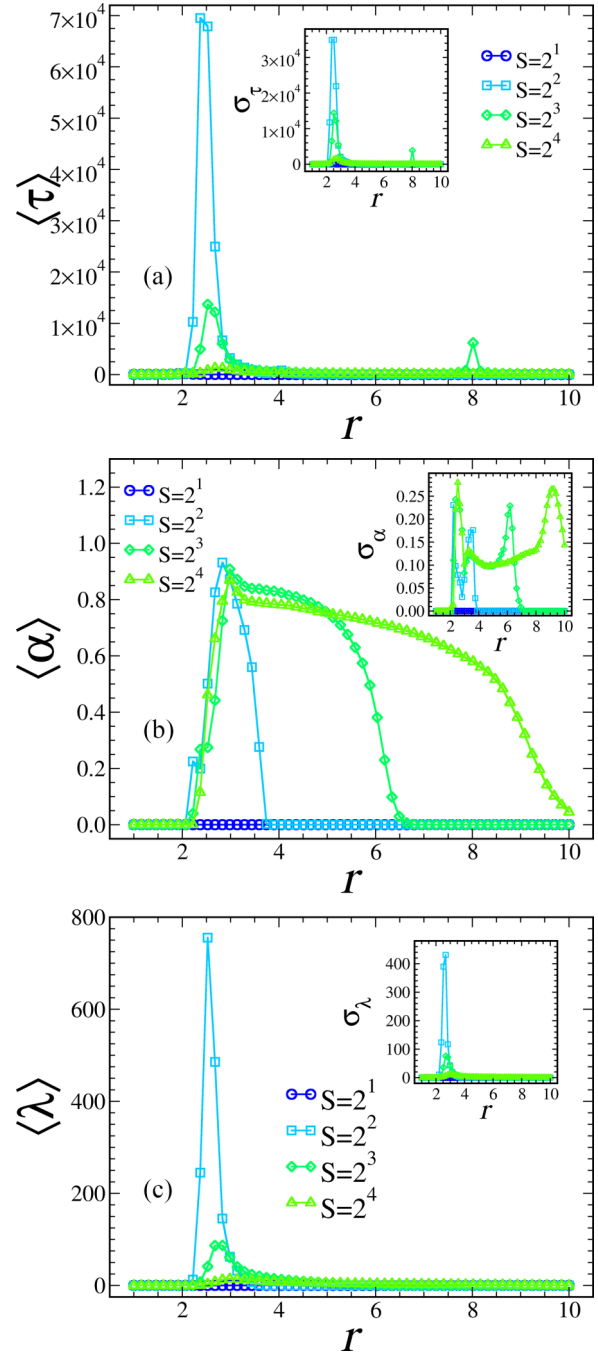


FIG. 5. Effect of the group size of the game on (a) the average time to reach an absorbing state, (b) the average time fraction with RPS cycles, and (c) the average number of cycles within the simulation time span as functions of r . Each point was obtained for a system of size $N = 8192$, averaging over 10^4 runs.

smaller sample sizes (S). Specifically, for $S = 2$, the system undergoes an abrupt crossover in the absorbing strategy from loner to cooperator, without any intermediate multistable state for the increment of the Δr used. For $S \geq 2^2$, there is a narrow region where cooperators remain the most likely absorbing state for $2 < r < 2.5$. However, near $r \approx 2.5$, the average absorbing time increases to approximately $\langle \tau \rangle = 7 \times 10^4$ MC steps, as shown in Fig. 5(a), with nearly half of the runs taking

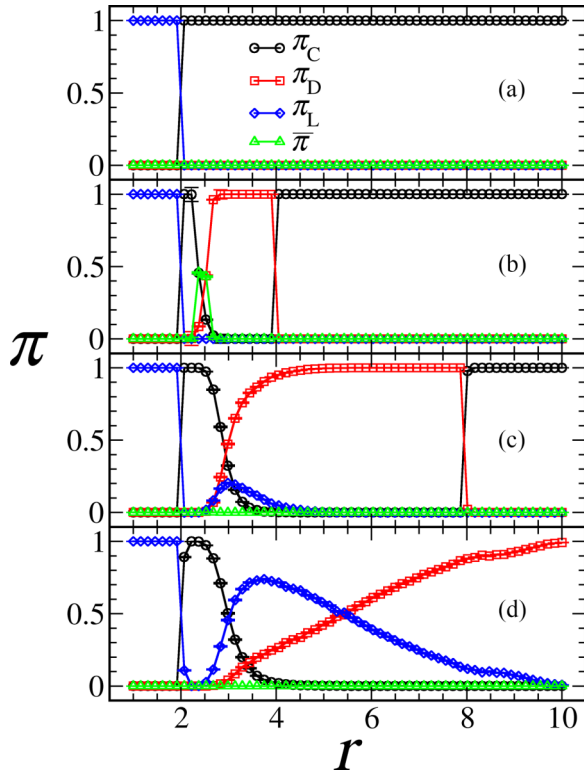


FIG. 6. Probabilities of reaching an absorbing state (or not) as functions of r for (a) $S = 2$, (b) $S = 2^2$, (c) $S = 2^3$, and (d) $S = 2^4$. Each point was obtained for a system of size $N = 8192$, averaging over 10^4 runs.

even longer, *i.e.* $\bar{\pi} \approx 0.5$. When $r \gtrsim 2.5$, defectors become the most likely absorbing state, coinciding with the peak of transient RPS cycles, which persist until $r \approx 3.9$ near where the expected abrupt crossover defector-cooperator occurs ($r \approx S$). After this value of r the RPS cycles vanish.

Finally, for $S \geq 2^3$ [see Figs. 6(c), 6(d)], the multistability of the absorbing states in the region $2 < r < S$ becomes smoother as the sizes of the sample groups increases. Specifically, when $S = 2^3$, the dynamics show cooperators decaying as absorbing strategy for $2.5 < r < 4$, with loners and defectors emerging as compelling strategies. Although for $S = 2^3$, loners have a peak at $r \approx 3$, defectors take over as the steady state strategy up until $r \approx S$. For $S = 2^4$, loners appear as the most likely absorbing strategy in the range of $3 \lesssim r \lesssim 5.5$. Additionally, larger sample groups exhibit a smoother transition in absorbing states.

Hauert *et al.* [40] have previously pointed to the fact that cooperation prevails when $r \geq S$, however, a more thorough explanation of this phenomenon is warranted. To understand the scenario in which voluntary cooperation becomes the prevailing strategy when the OPGG multiplication factor (r) is equal to the sampled group size (S), we first must realize that for this value of r , the loner strategy quickly disappears after a few MC steps. As a result, the sample group S reflects the participants in the public goods game.

Thus, let us consider two groups, A and B , each of size S . Group A consists of n defectors and $S - n$ cooperators, while group B is entirely made up of cooperators. So, the payoff for

a defector in group A is

$$\frac{(S - n)r}{S},$$

while the payoff of cooperators in B is $r - 1$. If a defector in the group A compares its payoff with any participant in the group B , it will shift to cooperation when the relation

$$\frac{(S - n)r}{S} < r - 1$$

is satisfied. That is, if $nr > S$. So, the critical situation for any number of defectors n occurs when $r = S$.

IV. CONCLUSION

We have conducted a detailed study of the conditions under which cooperation emerges in an optional public goods game (OPGG), demonstrating the emergence of cyclical dynamics akin to rock-paper-scissors interactions among the three possible strategies of the system. Our analysis reveals nonlinear, oscillatory behavior in the dynamics of cooperation, where each strategy dominates in turn within certain regions of key parameters, rather than the system settling into a fixed point. These transient cycles suggest that the conditions for the emergence and stabilization of cooperation are complex, with significant implications for understanding collective action in biological, social, and economic contexts.

Previous studies have attributed the emergence of cycles in OPGG to the inclusion of the third strategy, opting out of the game (loners), which introduces cyclic dominance. However, our findings demonstrate that while the inclusion of loners is necessary for this behavior, it is not sufficient on its own. For the spontaneous emergence of cycles, several nontrivial conditions must be met, which we summarize as follows:

(i) There are specific values of the parameter r that trigger rock-paper-scissors dynamics.

(ii) The group size S of participating players must be significantly smaller than the total population size ($S \ll N$).

(iii) The composition of each group changes at every iteration, ensuring no fixed interaction pattern. This setup mirrors the conditions of the social experiment reported in Ref. [20].

(iv) The absence of a local interaction structure, *i.e.*, the possibility for any agent to interact with any other within a fixed group size, makes the setup analogous to a mean-field approach, leading to the observed oscillations in strategy dominance.

It should be noted that additional mechanisms are also able to induce RPS cycles. In Ref. [28], the authors demonstrate that dilution and mobility in two-dimensional square lattices can also trigger this phenomenon. As a result, PGG, and even more so OPGG, are compelling protocols in game theory, and their theoretical investigations and applications warrant further exploration.

Some limitations of this study warrant further exploration. For instance, the multiplicative factor r could be modeled as a more elaborate function that accounts for seasonality, resource limitations, and the influence of noise over time. Future studies should also incorporate parameters that govern the evolution of other moral behaviors, such as truth telling [53], or more specifically, the dynamics of lying in mixed populations, gossip, and the development of trustworthiness [54].

Another important avenue for future research is the introduction of mechanisms involving fake cooperators to sustain cooperation within society. These agents, potentially introduced by governmental institutions, could help maintain cooperation levels and enhance the implementation of public goods.

Additionally, the study of goods with mixed capital—public and private—merits attention to improve the efficiency of public projects. This could include exploring tax exemptions or other mechanisms that facilitate the development and execution of such initiatives.

ACKNOWLEDGMENTS

E.V.S. thanks Conselho Nacional de Desenvolvimento Científico e Tecnológico of Brazil (CNPq) for supporting this work under Grant No. 153315/2024-5. S.G. and R.S. thank CNPq for partially supporting this work under Grants No. 314738/2021-5 and No. 304575/2022-4 respectively. J.R.I. acknowledges partial support from CNPq and the Instituto Nacional de Ciencia e Tecnologia de Sistemas Complexos. Additionally, we appreciate the availability of computational resources from the Lovelace cluster at IF-UFRGS.

-
- [1] S. Bowles and H. Gintis, *A Cooperative Species: Human Reciprocity and Its Evolution* (Princeton University Press, Princeton, 2011).
- [2] J. M. Smith, Evolutionary game theory, *Physica D* **22**, 43 (1986).
- [3] E. Fehr and K. M. Schmidt, A theory of fairness, competition, and cooperation, *Q. J. Econ.* **114**, 817 (1999).
- [4] G. E. Bolton and A. Ockenfels, Eric: A theory of equity, reciprocity, and competition, *Am. Econ. Rev.* **90**, 166 (2000).
- [5] M. N. Burton-Chellew and S. A. West, Payoff-based learning best explains the rate of decline in cooperation across 237 public-goods games, *Nat. Human Behav.* **5**, 1330 (2021).
- [6] O. Leimar and J. M. McNamara, Learning leads to bounded rationality and the evolution of cognitive bias in public goods games, *Sci. Rep.* **9**, 16319 (2019).
- [7] L. Andreozzi, M. Ploner, and A. S. Saral, The stability of conditional cooperation: beliefs alone cannot explain the decline of cooperation in social dilemmas, *Sci. Rep.* **10**, 13610 (2020).
- [8] K. De Jaegher, High thresholds encouraging the evolution of cooperation in threshold public-good games, *Sci. Rep.* **10**, 5863 (2020).
- [9] B. Battu and T. Rahwan, Cooperation without punishment, *Sci. Rep.* **13**, 1213 (2023).
- [10] A. M. Ibrahim, The conditional defector strategies can violate the most crucial supporting mechanisms of cooperation, *Sci. Rep.* **12**, 15157 (2022).
- [11] S. Podder and S. Righi, Complexity of behavioural strategies and cooperation in the optional public goods game, *Dyn. Games Appl.* **13**, 1219 (2023).
- [12] G. Charness and M. Rabin, Understanding social preferences with simple tests, *Q. J. Econ.* **117**, 817 (2002).
- [13] A. McAvoy, N. Fraiman, C. Hauert, J. Wakeley, and M. A. Nowak, Public goods games in populations with fluctuating size, *Theor. Popul. Biol.* **121**, 72 (2018).
- [14] V. Křivan and R. Cressman, Defectors' intolerance of others promotes cooperation in the repeated public goods game with opting out, *Sci. Rep.* **10**, 19511 (2020).
- [15] A. Rapaport and A. M. Chammah, *Prisoners Dilemma* (University of Michigan Press, Ann Arbor, MI, USA, 1965).
- [16] M. A. Nowak, Five rules for the evolution of cooperation, *Science* **314**, 1560 (2006).
- [17] D. G. Rand, A. Peysakhovich, G. T. Kraft-Todd, G. E. Newman, O. Wurzbacher, M. A. Nowak, and J. D. Greene, Social heuristics shape intuitive cooperation, *Nat. Commun.* **5**, 3677 (2014).
- [18] V. Capraro and M. Perc, Mathematical foundations of moral preferences, *J. R. Soc. Interface* **18**, rsif.2020.0880 (2021).
- [19] V. Capraro, J. Y. Halpern, and M. Perc, From outcome-based to language-based preferences, *J. Econ. Literature* **62**, 115 (2024).
- [20] U. Fischbacher and S. Gächter, Social preferences, beliefs, and the dynamics of free riding in public goods experiments, *Am. Econ. Rev.* **100**, 541 (2010).
- [21] E. Fehr and S. Gächter, Altruistic punishment in humans, *Nature (London)* **415**, 137 (2002).
- [22] R. Botta, G. Blanco, and C. E. Schaefer, Fractional punishment of free riders to improve cooperation in optional public good games, *Games* **12**, 17 (2021).
- [23] J. Li, Y. Liu, Z. Wang, and H. Xia, Egoistic punishment outcompetes altruistic punishment in the spatial public goods game, *Sci. Rep.* **11**, 6584 (2021).
- [24] A. Chaudhuri and T. Paichayontvijit, On the long-run efficacy of punishments and recommendations in a laboratory public goods game, *Sci. Rep.* **7**, 12286 (2017).
- [25] P. A. I. Forsyth and C. Hauert, Public goods games with reward in finite populations, *J. Math. Biol.* **63**, 109 (2011).
- [26] R. Botta, G. Blanco, and C. E. Schaefer, Discipline and punishment in panoptical public goods games, *Sci. Rep.* **14**, 7903 (2024).
- [27] W.-J. Li, Z. Chen, L.-L. Jiang, and M. Perc, Information sharing promotes cooperation among mobile individuals in multiplex networks, *Nonlinear Dyn.* **112**, 20339 (2024).
- [28] P. A. Valverde, R. da Silva, and E. V. Stock, Global oscillations in the optional public goods game under spatial diffusion, *Physica A* **474**, 61 (2017).
- [29] I. Okada, H. Yamamoto, E. Akiyama, and F. Toriumi, Cooperation in spatial public good games depends on the locality effects of game, adaptation, and punishment, *Sci. Rep.* **11**, 7642 (2021).
- [30] A. Civilini, O. Sadekar, F. Battiston, J. Gómez-Gardeñes, and V. Latora, Explosive cooperation in social dilemmas on higher-order networks, *Phys. Rev. Lett.* **132**, 167401 (2024).
- [31] Y. P. Ma, S. Gonçalves, S. Mignot, J.-P. Nadal, and M. B. Gordon, Cycles of cooperation and free-riding in social systems, *Eur. Phys. J. B* **71**, 597 (2009).
- [32] V. Capraro, A model of human cooperation in social dilemmas, *PLoS ONE* **8**, e72427 (2013).
- [33] A. Daniel, *Evolutionary Computation for Modeling and Optimization* (Springer, New York, 2006).
- [34] R. da Silva, A. L. Bazzan, A. T. Baraviera, and S. R. Dahmen, Emerging collective behavior and local properties of financial

- dynamics in a public investment game, *Physica A* **371**, 610 (2006).
- [35] R. da Silva, The public good game on graphs: Can the pro-social behavior persist? *Braz. J. Phys.* **38**, 74 (2008).
- [36] R. da Silva, L. F. Guidi, and A. Bararaviera, Mean field approximation for a stochastic public goods game, *Int. J. Bifurcation Chaos* **20**, 369 (2010).
- [37] K. Otten, U. J. Frey, V. Buskens, W. Przepiorka, and N. Ellemers, Human cooperation in changing groups in a large-scale public goods game, *Nat. Commun.* **13**, 6399 (2022).
- [38] C. Hauert, S. D. Monte, J. Hofbauer, and K. Sigmund, Volunteering as red queen mechanism for cooperation in public goods games, *Science* **296**, 1129 (2002).
- [39] D. Semmann, H.-J. Krambeck, and M. Milinski, Volunteering leads to rock–paper–scissors dynamics in a public goods game, *Nature (London)* **425**, 390 (2003).
- [40] C. Hauert, S. D. Monte, J. Hofbauer, and K. Sigmund, Replicator dynamics for optional public good games, *J. Theor. Biol.* **218**, 187 (2002).
- [41] C. Hauert and G. Szabo, Prisoner’s dilemma and public goods games in different geometries: Compulsory versus voluntary interactions, *Complexity* **8**, 31 (2003).
- [42] V. Capraro, J. J. Jordan, and D. G. Rand, Heuristics guide the implementation of social preferences in one-shot prisoner’s dilemma experiments, *Sci. Rep.* **4**, 6790 (2014).
- [43] C. Engel and L. Zhurakhovska, When is the risk of cooperation worth taking? The prisoner’s dilemma as a game of multiple motives, *Appl. Econ. Lett.* **23**, 1157 (2016).
- [44] R. M. Isaac and J. M. Walker, Group size effects in public goods provision: The voluntary contributions mechanism, *Q. J. Econ.* **103**, 179 (1988).
- [45] R. Isaac, J. M. Walker, and A. W. Williams, Group size and the voluntary provision of public goods: Experimental evidence utilizing large groups, *J. Public Econ.* **54**, 1 (1994).
- [46] H. Barcelo and V. Capraro, Group size effect on cooperation in one-shot social dilemmas, *Sci. Rep.* **5**, 7937 (2015).
- [47] M. Pereda, V. Capraro, and A. Sánchez, Group size effects and critical mass in public goods games, *Sci. Rep.* **9**, 5503 (2019).
- [48] A. Szolnoki and M. Perc, Group-size effects on the evolution of cooperation in the spatial public goods game, *Phys. Rev. E* **84**, 047102 (2011).
- [49] A. Traulsen, M. A. Nowak, and J. M. Pacheco, Stochastic payoff evaluation increases the temperature of selection, *J. Theor. Biol.* **244**, 349 (2007).
- [50] M. Perc, Coherence resonance in a spatial prisoner’s dilemma game, *New J. Phys.* **8**, 22 (2006).
- [51] G. Szabó and G. Fáth, Evolutionary games on graphs, *Phys. Rep.* **446**, 97 (2007).
- [52] J. Grujić, B. Eke, A. Cabrales, J. A. Cuesta, and A. Sánchez, Three is a crowd in iterated prisoner’s dilemmas: experimental evidence on reciprocal behavior, *Sci. Rep.* **2**, 638 (2012).
- [53] V. Capraro, M. Perc, and D. Vilone, The evolution of lying in well-mixed populations, *J. R. Soc. Interface* **16**, 20190211 (2019).
- [54] A. Kumar, V. Capraro, and M. Perc, The evolution of trust and trustworthiness, *J. R. Soc. Interface* **17**, 20200491 (2020).